

## Elastic properties of orthorhombic $\text{MgSiO}_3$ perovskite at lower mantle pressures

B.B. KARKI,<sup>1</sup> L. STIXRUDE,<sup>2</sup> S.J. CLARK,<sup>1</sup> M.C. WARREN,<sup>1</sup> G.J. ACKLAND,<sup>1</sup> AND J. CRAIN<sup>1</sup>

<sup>1</sup>Department of Physics and Astronomy, The University of Edinburgh, Edinburgh, EH9 3JZ, U.K.

<sup>2</sup>School of Earth and Atmospheric Sciences, Georgia Institute of Technology, Atlanta, Georgia 30332-0340, U.S.A.

### ABSTRACT

The full elastic constant tensor of orthorhombic  $\text{MgSiO}_3$  perovskite has been determined from first principles for the first time at high pressure using the plane-wave pseudopotential method. The athermal elastic moduli, determined throughout the pressure regime of the earth's mantle (0–140 GPa) from stress-strain relations, are found to be in excellent agreement with Brillouin scattering data at zero pressure. The degree of elastic anisotropy of the mineral is found to be strongly pressure dependent. The anisotropy at first decreases with pressure and then increases showing corresponding changes in the propagation directions of the slowest compressional (P) and shear (S) waves. Comparisons with seismological observations show that a Mg-rich silicate perovskite-dominated composition can plausibly account for the radial P- and S-wave velocity structure of the lower mantle.

### INTRODUCTION

Magnesium silicate perovskite has long been considered as the major constituent of the earth's lower mantle; the largest single region of the planet making up about 55% of its volume. Despite the geophysical significance of this mineral, our knowledge of its properties is limited, in most cases, to measurements at zero pressure. No experimental measurements of the elastic constants exist beyond ambient conditions (Yeganeh-Haeri 1994). Knowledge of the elastic constants at lower mantle pressures are particularly important geophysically as they determine the seismologically observable longitudinal (P) and shear (S) elastic wave velocities of this region.

Recent theoretical developments now make it possible to determine the elastic constants of  $\text{MgSiO}_3$  perovskite from first principles. These theoretical methods are completely independent of experiment and solve the quantum mechanical equations of density functional theory (Kohn and Sham 1965) with a minimum of approximations, using the plane-wave pseudopotential method. Difficulties faced by these elaborate electronic structure methods in the past, associated with the large unit cell and structural complexity of the orthorhombic ( $Pbnm$ ) structure, are now overcome by the implementation of an *ab initio* molecular dynamics technique that allows the structure to be efficiently optimized (Wentzcovitch et al. 1993; Warren and Ackland 1996; Karki et al. 1997a). Both plane-wave pseudopotential (Wentzcovitch et al. 1993) and linearized augmented plane-wave calculations (Stixrude and Cohen 1993) have shown that the orthorhombic phase is stable throughout the pressure regime of the lower mantle. Here we report the first-principles determination of the nine elastic stiffness coefficients of orthorhombic  $\text{MgSiO}_3$  perovskite at lower mantle pressures (up to 140 GPa) and discuss the geophysical implications of our results.

### METHODS

Our results are based on density functional theory (Kohn and Sham 1965) within the local density approximation (LDA) and pseudopotential theory (Payne et al. 1992). We use optimized norm-conserving, nonlocal pseudopotentials generated by the  $Q_c$  tuning method (Lin et al. 1993; Lee 1995) in the Kleinman-Bylander form (Kleinman and Bylander 1982). A plane-wave basis set is used with a cutoff energy of 850 eV, corresponding to approximately 9200 waves per band at each of four special  $k$  points (Monkhurst and Pack 1976). Finite basis set (Pulay) corrections to the total energies and the stresses (about 10 GPa at zero pressure) are included (Francis and Payne 1990; Karki et al. 1997a) so that the corrected energies and stresses are well converged.

In essence, determination of the elastic constants proceeds as follows. For a given pressure, we first determine the equilibrium structure of the 20-atom orthorhombic unit cell by minimizing the Hellman-Feynman forces and stresses acting respectively on the nuclei and the lattice parameters (Karki et al. 1997a; Wentzcovitch et al. 1993; Warren and Ackland 1996). The elastic constants are then determined by applying small strains and calculating the resulting stress tensor (Karki et al. 1997a; Nielsen and Martin 1985). Because strains couple to vibrational modes in the orthorhombic structure, the atomic positions are re-optimized in the strained configuration. Three orthorhombic and one shear (triclinic) strains are used to calculate the nine elastic moduli  $c_{11}$ ,  $c_{22}$ ,  $c_{33}$ ,  $c_{44}$ ,  $c_{55}$ ,  $c_{66}$ ,  $c_{12}$ ,  $c_{13}$ , and  $c_{23}$ . We vary the magnitude of the strain and derive the corresponding elastic constants from the resulting (non-linear) stress-strain relations as done by Karki et al. (1997a). This method has been applied previously to the determination of the elastic constants of  $\text{MgSiO}_3$  perovskite at zero pressure (Wentzcovitch et al. 1995) and

**TABLE 1.** Zero-pressure elastic moduli (GPa) of orthorhombic  $\text{MgSiO}_3$  perovskite compared with previous calculations and an experiment

	$C_{11}$	$C_{22}$	$C_{33}$	$C_{44}$	$C_{55}$	$C_{66}$	$C_{12}$	$C_{13}$	$C_{23}$	$K$	$G$
<b>Calculations</b>											
This study	487	524	456	203	186	145	128	144	156	258	175
Wentzcovitch et al. (1995)	496	560	504	151	198	171	132	136	156	267	179
Cohen (1987)	548	551	441	241	253	139	54	153	175	256	196
Matsui et al. (1987)	460	506	378	162	159	112	139	184	177	260	140
<b>Experiment</b>											
Yeganeh-Haeri (1994)	482(4)	537(3)	485(5)	204(2)	186(2)	147(3)	144(6)	147(6)	146(7)	264(5)	177(4)

those of  $\text{MgO}$  and  $\text{SiO}_2$  at high pressure (Karki et al. 1997a, 1997b). In all cases, the results have been found to compare favorably with available experimental data.

### RESULTS

The structure of magnesium silicate perovskite consists of a corner-linked network of  $\text{SiO}_6$  octahedra, with Mg atoms surrounded by cages of eight octahedra. The stable orthorhombic ( $Pbnm$ ) phase differs from the ideal cubic polytype ( $Pm3m$ ) in that the octahedra are distorted and rotated about the crystallographic axes, and the Mg atoms are displaced from the centers of the octahedral cages. Our calculated structural parameters (three cell and seven internal) of orthorhombic  $\text{MgSiO}_3$  perovskite at zero pressure are  $a = 4.789$ ,  $b = 4.922$ , and  $c = 6.893$  Å; and  $\text{Mgx} = 0.5129$ ,  $\text{Mgy} = 0.5521$ ,  $\text{O1x} = 0.0980$ ,  $\text{O1y} = 0.4686$ ,  $\text{O2x} = 0.1983$ ,  $\text{O2y} = 0.2033$ , and  $\text{O2z} = 0.5507$  compared to corresponding values of 4.779, 4.932, and 6.908 Å; and 0.5141, 0.5560, 0.1028, 0.4660, 0.1961, 0.2014, and 0.5531, respectively, from experiment (Horieuchi et al. 1987). As at zero pressure, the calculated lattice parameters of perovskite at higher pressures are with-

in 1% of the experiments (Mao et al. 1991; Ross and Hazen 1990; Knittle and Jeanloz 1987).

The predicted elastic constants of  $\text{MgSiO}_3$  perovskite at zero pressure are in better agreement with measurements (Yeganeh-Haeri 1994) than the previous calculations (Wentzcovitch et al. 1995; Matsui et al. 1987; Cohen 1987) (Table 1). The relatively high values of the elastic moduli compared with other silicates reflect the dense packing of the perovskite structure and the rigidity of the  $\text{SiO}_6$  octahedra, which form a corner-sharing three-dimensional network. Differences between the present and previous pseudo potential calculations (Wentzcovitch et al. 1995) are attributed to the nonlinearity of the stress-strain relations (which we have taken into account) and to more extensive sampling of the irreducible wedge of the Brillouin zone of our study. The fact that both pseudopotential results are substantially better than the predictions based on semi-empirical rigid-ion or ab initio modified-electron-gas models (Matsui et al. 1987; Cohen 1987) indicates an important influence of covalent forces on the elasticity of silicate perovskite. Figure 1 shows the pressure variations of the calculated elastic moduli. We find at zero pressure  $c_{22} > c_{11} > c_{33}$ , whereas Brillouin scattering data (Yeganeh-Haeri 1994) show  $c_{22} > c_{33} > c_{11}$ , as do previous pseudopotential results (Wentzcovitch et al. 1995). However, our results are consistent with static compression data (Mao et al. 1991), which find that the  $c$  axis is most compressible and the  $b$  axis least compressible at low pressure. Above 20 GPa, we find  $c_{22} > c_{33} > c_{11}$ , indicating that the  $a$  axis is the most compressible at higher pressures.

$\text{MgSiO}_3$  perovskite is elastically anisotropic as indicated by its three different axial compressibilities. We calculated the single-crystal elastic wave velocities in different directions (Karki et al. 1997a) and found that the azimuthal anisotropy of shear (S) waves ( $A_s$ ) is much stronger than that of compressional (P) waves ( $A_p$ ) (Fig. 2). At zero pressure, the maximum and minimum longitudinal and shear velocities differ by 8 and 17%, respectively, consistent with the results of Yeganeh-Haeri (1994) (7 and 18%, respectively), whereas at 140 GPa the P- and S-wave velocities vary with propagation direction by 12 and 21%, respectively. The maximum polarization anisotropy of the shear waves varies from 17% at zero pressure to 14% at 140 GPa (Fig. 2). The pressure dependence of the anisotropy is not monotonic: The changes in the pressure dependence (at about 20 and

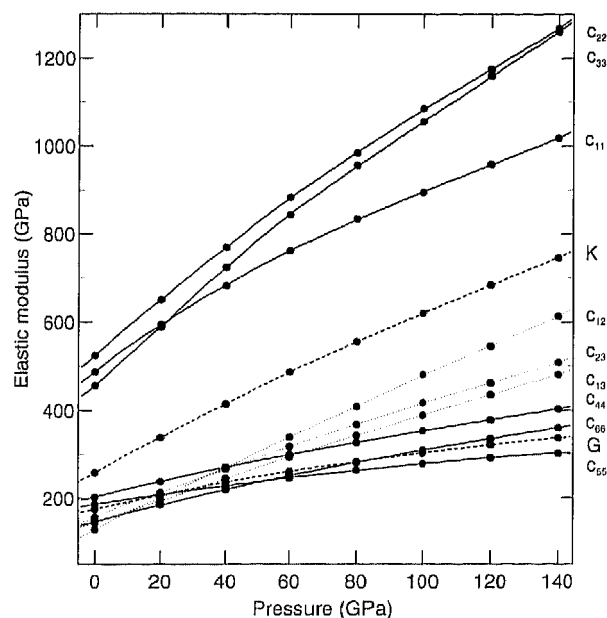


**FIGURE 1.** Pressure variation of elastic moduli (lines with symbols) of orthorhombic  $\text{MgSiO}_3$  perovskite.

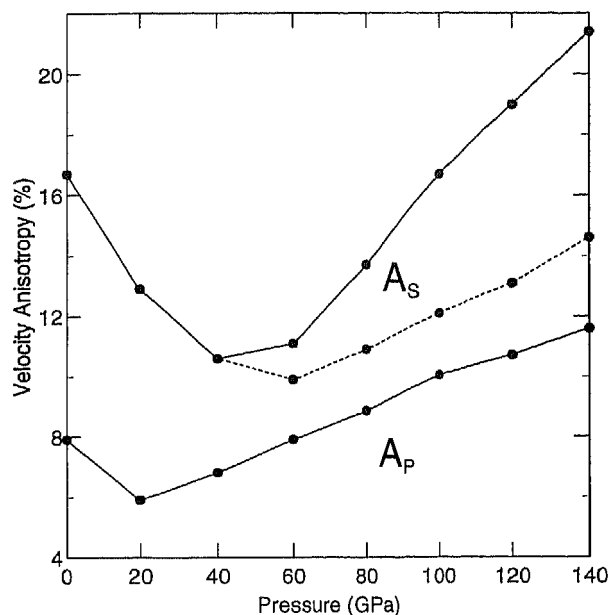


FIGURE 2. Pressure dependence of azimuthal anisotropy (solid line) of compressional wave velocity ( $A_p$ ) and azimuthal (solid line) and polarization (dashed line) anisotropy of the shear wave velocity ( $A_s$ ) of MgSiO<sub>3</sub> perovskite:

$$A = \frac{V_{\max} - V_{\min}}{V_{\text{avg}}} \times 100;$$

where  $V_{\text{avg}}$  represents the isotropic value.

40 GPa for  $A_p$  and  $A_s$ , respectively) are reflected in changes in the slowest propagation directions of the P- and S-waves beyond 20 and 40 GPa, respectively. At 0 GPa, the fastest and slowest longitudinal waves propagate along [011] and [001], respectively, whereas the fastest and slowest shear waves both propagate along [010] and are polarized in the (001) and (100) planes, respectively. However, at 140 GPa, the longitudinal and shear waves are slowest along [100] and [110], respectively, and the direction of maximum polarization S-wave anisotropy is [001].

We computed the elastic properties of an isotropic polycrystalline aggregate from the elastic constants by using the Hill averaging scheme (Hill 1952). At zero pressure, the isotropic bulk and shear moduli are  $K_0 = 258$  and  $G_0 = 175$  GPa, in excellent agreement with experimental and previous pseudopotential results (Table 1). The differences between the upper (Voigt) and lower (Reuss) bounds for the bulk and shear moduli are 0.5 and 2.5 GPa, respectively, at zero pressure, and 8.0 and 10.2 GPa at 140 GPa. Figure 3 shows the calculated compressional (P) and shear (S) wave velocities,  $V_p$  and  $V_s$ , respectively, using

$$V_p = \sqrt{\frac{K + \frac{4}{3}G}{\rho}} \quad \text{and} \quad V_s = \sqrt{\frac{G}{\rho}}$$

where  $\rho$  is the density.

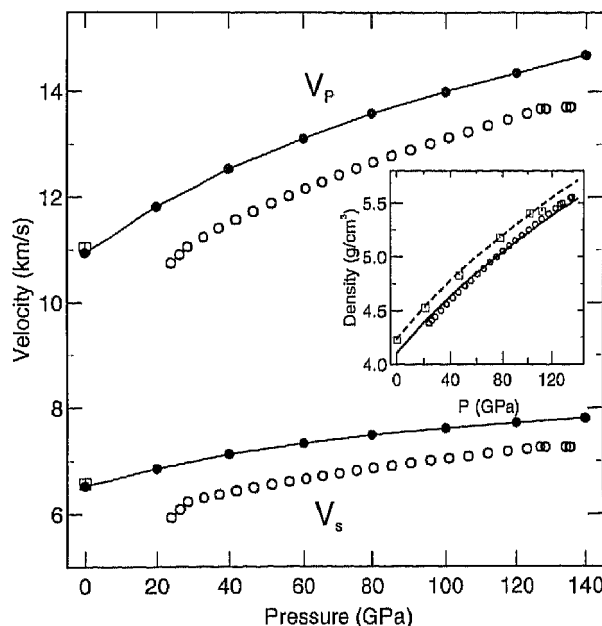


FIGURE 3. Isotropic wave velocities,  $V_p$  and  $V_s$ , of MgSiO<sub>3</sub> perovskite. Calculated velocities (solid lines with solid circles) are compared with the seismic values (open circles) from Dziewonski and Anderson (1981). The ambient pressure velocities (squares) are from Brillouin spectroscopy (Yeganeh-Haeri 1994). The inset compares theoretical (solid line) with seismic (open circles) and experimental (squares, Knittle and Jeanloz 1987) values of density. The dashed line represents the theoretical result corrected for 10% Fe content (Duffy and Anderson 1989).

### GEOPHYSICAL IMPLICATIONS

Our calculations allow, for the first time, the comparison of the high-pressure density, P- and S-wave velocities, and elastic anisotropy of MgSiO<sub>3</sub> perovskite with observed lower mantle seismic properties. Comparison with the spherically averaged (radial) structure of the lower mantle (Dziewonski and Anderson 1981) shows that our theoretical P- and S-wave velocity curves are essentially parallel with those of the lower mantle (Fig. 3). Moreover, predicted elastic wave velocities are similar in magnitude to those observed: Theoretical P- and S-wave velocities are 6 and 8% higher, respectively, than those observed seismologically (Fig. 3). These results are consistent with a lower mantle mineralogy dominated by Mg-rich silicate perovskite. The small differences between theoretical and observed seismic velocities can be explained by the presence of Fe in the lower mantle (expected to reduce velocities by 1–2%), and the high temperature of the lower mantle (2000–3000 K), which is expected to reduce velocities by several percent from their zero temperature values (Duffy and Anderson 1989). The possible presence of secondary phases in the lower mantle (e.g., magnesiowüstite, CaSiO<sub>3</sub> perovskite) may also contribute to the difference between predicted and observed seismic velocities.

Our results are an important test of the prevailing view

that Mg-rich silicate perovskite is the most abundant mineral in the lower mantle. This picture has been supported in the past by only a limited set of seismological observations: the density and bulk sound velocity (Bukowski 1990, Stixrude et al. 1992; Yeganeh-Haeri 1994). The present results show for the first time that the properties of perovskite sensitive to the shear modulus, such as  $V_p$  and  $V_s$ , are also consistent with seismological observations of the lower mantle.

Our prediction that  $\text{MgSiO}_3$  perovskite remains significantly anisotropic throughout the pressure regime of the lower mantle bears on seismic observations of anisotropy (Karato 1997). Shear-wave splitting observations show no detectable polarization anisotropy throughout the bulk of the lower mantle (Meade et al. 1995). Our results then imply that anisotropic single crystals of perovskite must be randomly oriented in the lower mantle, that is, the preferred orientation (texture) in this region must be weak. The isotropy of the bulk of the lower mantle contrasts sharply with that of the upper and lower few hundred kilometers of the mantle. Our predictions of single-crystal elastic wave velocities of perovskite and their pressure dependence will be relevant for interpreting observations of anisotropy in the D'' region at the base of the mantle (Kendall and Silver 1996).

#### ACKNOWLEDGMENTS

The authors thank EPSRC for computing facilities under grant GRIK74067, M.C. Payne for the original CASTEP code, and M.H. Lee for pseudopotentials. B.B.K. acknowledges support from the Premier Scholarship from the University of Edinburgh. L.S. is supported by the National Science Foundation under grant EAR-9305060. M.C.W. and S.J.C. thank the EPSRC for support. J.C. acknowledges support from the Royal Society of Edinburgh.

#### REFERENCES CITED

- Bukowski, M.S.T. and Wolf, G.H. (1990) Thermodynamically consistent decompression: Implications for the lower mantle composition. *Journal of Geophysical Research*, 95, 12583–12593.
- Cohen, R.E. (1987) Elasticity and equation of state of  $\text{MgSiO}_3$ -perovskite. *Geophysical Research Letters*, 14, 1053–1056.
- Duffy, T.S. and Anderson, D.L. (1989) Seismic velocities in mantle minerals and the mineralogy of the upper mantle. *Journal of Geophysical Research*, 94, 1895–1912, 1989.
- Dziewonski, A.M. and Anderson, O.L. (1981) Preliminary reference earth model. *Physics of Earth and Planetary Interiors*, 25, 297–356.
- Francis, G.P. and Payne, M.C. (1990) Finite basis set corrections to total-energy pseudopotential calculations. *Journal of Physics, Condensed Matter*, 2, 4395–4404.
- Hill, R. (1952) The elastic behaviour of a crystalline aggregate. *Proceedings Physical Society London*, 65A, 349–354.
- Horiuchi, H., Ito, E., and Weidner, D. (1987) Perovskite type  $\text{MgSiO}_3$ : single crystal X-ray diffraction study. *American Mineralogist*, 72, 357–360.
- Karato, S. (1997) Seismic anisotropy in the deep mantle, boundary layers and geometry of mantle convection. *Pure and Applied Geophysics*, in press.
- Karki, B.B., Stixrude, L., Clark, S.J., Warren, M.C., Ackland, G.J., and Crain, J. (1997a) Structure and elasticity of MgO at high pressure. *American Mineralogist*, 82, 51–60.
- Karki, B.B., Warren, M.C., Stixrude, L., Ackland, G.J., and Crain, J. (1997b) *Ab initio* studies of high-pressure structural transformations in silica. *Physical Review B*, 55, 3465–3472.
- Kendall, J.M. and Silver, P.G. (1996) Constraints from seismic anisotropy on the nature of the lowermost mantle. *Nature*, 381, 409–412.
- Kleinman, L. and Bylander, D.M. (1982) Efficacious form for model pseudopotentials. *Physical Review Letters*, 48, 1425–1428.
- Knittle, E. and Jeanloz, R. (1987) Synthesis and equation of state of  $(\text{Mg,Fe})\text{SiO}_3$  perovskite to over 100 Gigapascals. *Science*, 235, 668–670.
- Kohn, W. and Sham, L.J. (1965) Self-consistent equations including exchange and correlation effects. *Physical Review*, 140, A1133–A1138.
- Lee, M.H. (1995) Advanced pseudopotentials for large scale electronic structure calculations. Ph.D Thesis, University of Cambridge, U.K.
- Lin, J.S., Qteish, A., Payne, M.C., and Heine, V. (1993) Optimised and transferable non-local separable *ab initio* pseudopotentials. *Physical Review B*, 47, 4174–4180.
- Mao, H.K., Hemley, R.J., Fei, Y., Shu, J.F., Chen, L.C., Jephcoat, A.P., Wu, Y., and Bassett, W.A. (1991) Effect of pressure, temperature, and composition on lattice parameters and density of  $(\text{Fe,Mg})\text{SiO}_3$ -perovskites to 30 GPa. *Journal of Geophysical Research*, 96, 8069–1079.
- Matsui, M., Akaogi, M., and Matsumoto, T. (1987) Computational model of the structural and elastic properties of the ilmenite and perovskite phases of  $\text{MgSiO}_3$ . *Physics and Chemistry of Minerals*, 14, 101–106.
- Meade, C., Silver, P.G., and Kaneshima, S. (1995) Laboratory and seismological observations of lower mantle isotropy. *Geophysical Research Letters*, 22, 1293–1296.
- Monkhurst, H.J. and Pack, J.D. (1976) Special points for Brillouin-zone integrations. *Physical Review B Solid State*, 13, 5188–5192.
- Nielsen, O.H. and Martin, R. (1985) Quantum mechanical theory of stress and force. *Physical Review B*, 32, 3780–3791.
- Payne, M.C., Teter, M.P., Allen, D.C., Arias, T.A., and Joannopoulos, J.D. (1992) Iterative minimisation techniques for *ab initio* total-energy calculations: molecular dynamics and conjugate gradients. *Reviews of Modern Physics*, 64, 1045–1097.
- Ross, N.L. and Hazen, R.M. (1990) High-pressure crystal chemistry of  $\text{MgSiO}_3$  perovskite. *Physics and Chemistry of Minerals*, 17, 228–237.
- Stixrude, L., Hemley, R.J., Fei, Y., and Mao, H.-K. (1992) Thermoelasticity of silicate perovskite and magnesiowustite and the stratification of the earth's mantle. *Science*, 257, 1099–1101.
- Stixrude, L. and Cohen, R.E. (1993) Stability of orthorhombic  $\text{MgSiO}_3$ -perovskite in the Earth's lower mantle. *Nature*, 364, 613–616.
- Warren, M.C. and Ackland, G.J. (1996) *Ab initio* studies of structural instabilities in magnesium silicate perovskite. *Physics and Chemistry of Minerals*, 23, 107–118.
- Wentzcovitch, R.M., Martins, J.L., and Price, G.D. (1993) *Ab initio* molecular dynamics with variable cell shape: application to  $\text{MgSiO}_3$  perovskite. *Physical Review Letters*, 70, 3947–3950.
- Wentzcovitch, R.M., Ross, N.L., and Price, G.D. (1995) *Ab initio* study of  $\text{MgSiO}_3$  and  $\text{CaSiO}_3$  perovskites at lower mantle pressures. *Physics of Earth and Planetary Interiors*, 90, 101–112.
- Yeganeh-Haeri, A. (1994) Synthesis and re-investigation of the elastic properties of single-crystal magnesium silicate perovskite. *Physics of Earth and Planetary Interiors*, 87, 111–121.

MANUSCRIPT RECEIVED JANUARY 23, 1997

MANUSCRIPT ACCEPTED MARCH 13, 1997